AUT Journal of Mechanical Engineering

AUT J. Mech. Eng., 2(1) (2018) 91-98
DOI: 10.22060/ajme.2018.12951.5485

Effect of Concentrated Axial Harmonic Force on Lateral Vibration of a Mono- Disk Rotating Shaft

M. R. Zeinolabedini, M. Rafeeyan*

Department of Mechanical Engineering, Yazd University, Yazd, Iran

ABSTRACT: Rotor vibrations and its control is an important subject in many industries such as power plants and gas stations. When lateral vibrations of rotors during operation exceeds allowable level, a huge damage will be occurred. Surge and stall may be some common reasons of these vibrations. This paper aims to present a simple model for surge and stall and assumes that its effect as a concentrated force acting on a rotor-disk system. This is a basic and conceptual model for future investigations in this area. Therefore, the effect of a concentrated axial force exerted on an assembled disk on a rotating shaft is investigated theoretically. Equations of motion are derived using Timoshenko beam theory. This governing equations consist of four coupled partial differential equations. Since these equations are complex, coupled and have time-varying coefficients, they are solved using a combination of Galerkin and Newmark methods. Numerical examples are analyzed as well. The accuracy of these equations is verified for a simple beam. Results indicate that the axial load has a considerable effect on the lateral vibration amplitude of the rotor and this simple proposed model can be improved for next studies in this area.

Review History:

Received: 3 June 2017
Revised: 24 December 2017
Accepted: 2 January 2018
Available Online: 1 March 2018

Keywords:

Axial load
Rotor Vibration
Surge
Stall
Galerkin method

1- Introduction

Rotor Dynamics is a branch of dynamic systems dealing with Rotor systems are widely used assemblies for power transmission in various kinds of machinery. The lateral vibrations of the rotors must be limited because excessive vibrations will affect the running status of it and may lead to catastrophic accidents. Due to several factors, which contribute to the energy transfer, the rotor rotations generate different modes of vibrations: lateral, torsional and axial modes. Among these modes, the lateral is of the greatest concern [1]. The simplest model that can be adopted to study the flexible behavior of rotors consists of a point mass attached to a massless shaft, often referred to as Jeffcott rotor. Rotors of turbines and compressors carry one or more disks. When flexible rotors are assessed it is a common practice to neglect axial forces and the interaction between these forces and radial vibration.

In general, axial forces are indeed small therefore are not considered. In aircraft engines, the thrust generates axial force in the rotor system. In compressors stall and surge phenomena can generate horizontal force on disks. These forces may be constant, while in rotating machinery is specific, they may be harmonic or random. This is the main motivation of current research.

Nelson et al. [2] Studied the vibration analysis of the Timoshenko rotor with internal damping subject to axial load. Edney et al. [3] presented the dynamic analysis of the tapered Timoshenko rotor. Chen et al. [4] analyzed an exact and direct modeling technique for rotor bearing system subject to axial load. Choi et al. [5] presented the consistent derivation of a set of governing differential equations describing the vibration in two orthogonal planes and the torsional vibration of a straight rotor with dissimilar lateral principle moments of inertia, subject to a constant compressive axial load. Huajian Gouyang et al. [6] presented a dynamic model for the vibration of a rotating Timoshenko beam subjected to a three- directional load moving in the axial direction. Askarian et al. [7] assessed the effect of various parameters like axial force, unbalance, and coupling misalignment on vibration of a rotor. Nawal H.Al et al. [8] derived the equation of motion that governs the transvers vibration of a beam loaded axially and compared the natural frequencies thereof. Motallebi et al. [9] adopted a homotopy analysis based method to assess the vibration of a nonlinear beam subject to axial force. Torabi et al. [10] presented an analytical solution for whirling analysis of axial-loaded Timoshenko rotor and corresponding basic function.

In this study the dynamics of a rotating shaft, modeled as a Timoshenko rotor, subject to concentrated harmonic load acting on the surface of a disk on the rotor is investigated. For this, the dynamic equations of lateral vibrations of the rotor are derived using Timoshenko beam model and Newton's second law. Then, this governing equations are solved by Galerkin and Newmark method. Then, numerical simulations are carried out and the effects of force magnitude are analyzed.

2- Governing Equations and Solution Procedure

A simply supported Timoshenko rotor subject to axial force acted on a disk is shown in Fig. 1.

As observed in Fig. 2 bending moment is due to concentrated load:

Corresponding author, E–mail: Rafeeyan@yazd.ac.ir

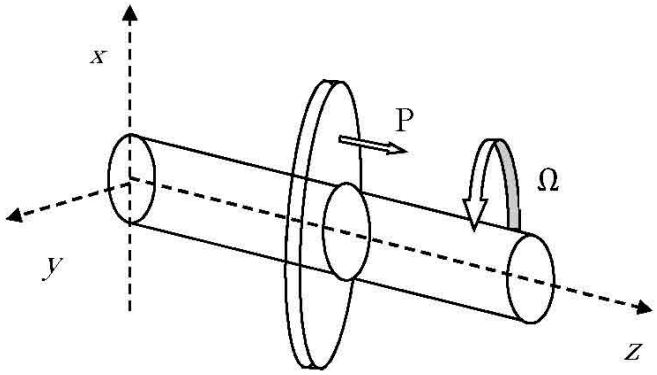

Fig. 1. Rotating Timoshenko shaft with an axial loaded disk

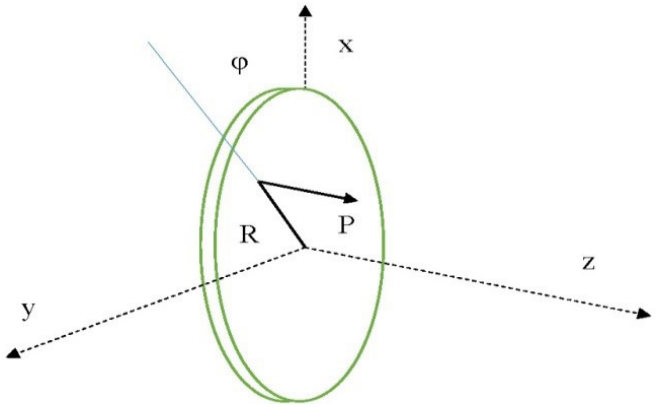

Fig. 2. Concentrated load position on the disk

$$m_x = PR\cos\varphi\delta(z-z_0)$$
$$m_y = PR\sin\varphi\delta(z-z_0) \quad (1)$$

where, R is the radius of the force point and ∅ is the angle of the force with x axis.
By applying the equilibrium of forces and momentums, the set of equations of motion are extracted as follows:

$$F_x + \frac{\partial F_x}{\partial z}dz - F_x + \left(P + \frac{\partial P}{\partial z}dz\right)\left(\frac{\partial u_x}{\partial z} + \frac{\partial^2 u_x}{\partial z^2}dz\right)$$
$$-P\frac{\partial u_x}{\partial z} + f_x(x,t) = \left[\rho A + M_0\delta(z-z_0)\right]dz\,\frac{\partial^2 u_x}{\partial t^2}$$
$$F_y + \frac{\partial F_y}{\partial z}dz - F_y + \left(P + \frac{\partial P}{\partial z}dz\right)\left(\frac{\partial u_y}{\partial z} + \frac{\partial^2 u_y}{\partial z^2}dz\right)$$
$$-P\frac{\partial u_y}{\partial z} + f_y(x,t) = \left[\rho A + M_0\delta(z-z_0)\right]dz\,\frac{\partial^2 u_y}{\partial t^2}$$
$$M_x + \frac{\partial M_x}{\partial z}dz - M_x - \left(F_y + \frac{\partial F_y}{\partial z}dz\right)dz + m_x = \quad (2)$$
$$\left[\rho I_x + I_x\delta(z-z_0)\right]\frac{\partial^2\varphi_x}{\partial t^2}dz$$
$$+\left[\rho I_p + I_p\delta(z-z_0)\right]\Omega dz\,\frac{\partial\varphi_y}{\partial t}$$
$$M_y + \frac{\partial M_y}{\partial z}dz - M_y - \left(F_x + \frac{\partial F_x}{\partial z}dz\right)dz + m_y =$$
$$\left[\rho I_y + I_y\delta(z-z_0)\right]\frac{\partial^2\varphi_y}{\partial t^2}dz$$
$$+\left[\rho I_p + I_p\delta(z-z_0)\right]\Omega dz\,\frac{\partial\varphi_x}{\partial t}$$

Where u_x , u_y , φ_x and φ_y are components of displacement and rotation in x and y directions, respectively; ρ is mass density. In addition A, I_x , I_y and I_p are cross- sectional area, moment of inertia about the x and y axes and polar moment of inertia, respectively; f_x and f_y and P are forces per unit length in x and y directions and axial force.
According to Timoshenko beam theory, components of bending moment (M) and shear force (F) in x and y directions are presented as follows [11]:

$$F_x = kGA\left(\frac{\partial u_x}{\partial z} - \varphi_y\right)$$
$$F_y = kGA\left(\frac{\partial u_y}{\partial z} - \varphi_x\right) \quad (3)$$
$$M_x = EI_x\frac{\partial\varphi_x}{\partial z}$$
$$M_y = EI_y\frac{\partial\varphi_y}{\partial z}$$

Were E and G are the modulus of elasticity and shear modulus, respectively; k is the shear correction factor depending on the shape of the section and Poisson's ratio of material [12]. By neglecting the term of $(dz)^2$ and using the following relation for a circular section

$$I_p = 2I_x = 2I_y = 2I \quad (4)$$

Eq.(2) can be written as:

$$kAG\left(\frac{\partial^2 u_x}{\partial z^2} - \frac{\partial\varphi_y}{\partial z}\right) + \frac{\partial}{\partial z}\left(P\frac{\partial u_x}{\partial z}\right) + f_x(x,t) =$$
$$\left[\rho A + M_0\delta(z-z_0)\right]\frac{\partial^2 u_x}{\partial t^2}$$
$$kAG\left(\frac{\partial^2 u_y}{\partial z^2} - \frac{\partial\varphi_x}{\partial z}\right) + \frac{\partial}{\partial z}\left(P\frac{\partial u_y}{\partial z}\right) + f_y(x,t) =$$
$$\left[\rho A + M_0\delta(z-z_0)\right]\frac{\partial^2 u_y}{\partial t^2} \quad (5)$$
$$EI\frac{\partial^2\varphi_x}{\partial Z^2} - kGA\left(\frac{\partial u_y}{\partial Z} + \varphi_x\right) + m_x =$$
$$\left[\rho I + I\delta(z-z_0)\right]\frac{\partial^2\varphi_x}{\partial t^2} + 2\left[\rho I + I_0\delta(z-z_0)\right]\Omega\frac{\partial\varphi_y}{\partial t}$$
$$EI\frac{\partial^2\varphi_y}{\partial z^2} - kGA\left(\frac{\partial u_x}{\partial z} + \varphi_y\right) + m_y =$$
$$\left[\rho I + I_0\delta(z-z_0)\right]\frac{\partial^2\varphi_y}{\partial t^2} + 2\left[\rho I + I_0\delta(z-z_0)\right]\Omega\frac{\partial\varphi_x}{\partial t}$$

where, R_0 and P_0 are the reaction of force in the support and axial force exerted on disk.
The force at the cross-section of the rotor is written as:

$$P(z,t) = -R_0 - P_0(t)H(z-z_0) \quad (6)$$

By re-arranging, the equations of motion can be written:

$$
\begin{aligned}
&kGA\left(\frac{\partial^2 u_x}{\partial z^2}+\frac{\partial \varphi_x}{\partial z}\right)-\left[R_0+P_0(t)H(z-z_0)\right]\frac{\partial^2 u_x}{\partial z^2}\\
&-P_0(t)H(z-z_0)\frac{\partial u_x}{\partial z}+f_x(x,t)=\\
&\left[\rho A+M_0\delta(z-z_0)\right]\frac{\partial^2 u_x}{\partial t^2}\\
&kGA\left(\frac{\partial^2 u_y}{\partial z^2}+\frac{\partial \varphi_y}{\partial z}\right)-\left[R_0+P_0(t)H(z-z_0)\right]\frac{\partial^2 u_y}{\partial z^2}\\
&-P_0(t)\delta(z-z_0)\frac{\partial u_y}{\partial z}+f_y(x,t)=\\
&\left[\rho A+M_0\delta(z-z_0)\right]\frac{\partial^2 u_y}{\partial t^2}\\
&EI\frac{\partial^2 \varphi_x}{\partial z^2}-kGA\left(\frac{\partial u_y}{\partial z}+\varphi_x\right)\\
&+PR\cos\varphi\,\delta(z-z_0)=\left[\rho I+I_0\delta(z-z_0)\right]\frac{\partial^2 \varphi_x}{\partial t^2}\\
&+2\left[\rho I+I_0\delta(z-z_0)\right]\Omega\frac{\partial \varphi_y}{\partial t}\\
&EI\frac{\partial^2 \varphi_y}{\partial z^2}+kGA\left(\frac{\partial u_x}{\partial z}-\varphi_y\right)+PR\sin\varphi\,\delta(z-z_0)=\\
&\left[\rho I+I_0\delta(z-z_0)\right]\frac{\partial^2 \varphi_y}{\partial t^2}+2\left[\rho I+I_0\delta(z-z_0)\right]\Omega\frac{\partial \varphi_x}{\partial t}
\end{aligned}
\tag{7}
$$

By introducing the following complex variables:

$$
\begin{aligned}
u&=u_x+ju_y\\
\varphi&=\varphi_x+j\varphi_y\\
f&=f_x+jf_y
\end{aligned}
\tag{8}
$$

and the external forces consisting weight and unbalanced force written as:

$$
\begin{aligned}
&f(x,t)=f_1(x,t)+f_2(x,t)=\rho Ag-\\
&[M_0 g\,\delta(z-z_0)+\\
&\Omega^2 e_0 m_0^p\left[\cos(\Omega t+\theta_0)+j\sin(\Omega t+\theta_0)\right]\delta(z-z_0)]
\end{aligned}
\tag{9}
$$

where, M_0 is the disk mass, m_0^p is the unbalanced mass, e_0 is the unbalanced radius and θ_0 is the angle of unbalanced mass with respect to horizontal axis, the following set of equations of motion is yield:

$$
\begin{aligned}
&-\left[\rho A+M_0\delta(z-z_0)\right]\frac{\partial^2 u}{\partial t^2}+kGA\left(\frac{\partial^2 u}{\partial z^2}+j\frac{\partial \varphi}{\partial z}\right)\\
&-\left[R_0+P_0(t)H(z-z_0)\right]\frac{\partial^2 u}{\partial z^2}-P_0(t)\delta(z-z_0)\frac{\partial u}{\partial z}\\
&=\rho Ag+\left[P_0M_0g-m_0^p\Omega\cos(\Omega t+\theta_0)\right]\delta(z-z_0)\\
&-j\Omega m_0^p\sin(\Omega t+\theta_0)\delta(z-z_0)\\
&-\left[\rho I+I_0\delta(z-z_0)\right]\frac{\partial^2 \varphi}{\partial t^2}\\
&+2j\left[\rho I+I_0\delta(z-z_0)\right]\Omega\frac{\partial \varphi}{\partial t}+EI\frac{\partial^2 \varphi}{\partial z^2}\\
&-kGA\left(\varphi-j\frac{\partial u}{\partial z}\right)=PRe^{-J\varphi}\delta(Z-Z_0)
\end{aligned}
\tag{10}
$$

For a rotor with simple support the following equation must be met:

$$
\begin{aligned}
&z=0:u=0,\frac{\partial \varphi}{\partial z}=0\\
&z=L:u=0,\frac{\partial \varphi}{\partial z}=0
\end{aligned}
\tag{11}
$$

The solution of Eq.10 is assumed as:

$$
\begin{aligned}
u(z,t)&=\sum_{n=1}^{\infty}a_n(t)\sin(\frac{n\pi z}{L})\\
\varphi(z,t)&=\sum_{n=1}^{\infty}b_n(t)\cos\left[\frac{(n-1)\pi z}{L}\right]
\end{aligned}
\tag{12}
$$

Inserting Eq.12 into Eq.10 and then running the required simplifications the following equations are obtained:

$$
\begin{aligned}
&\sum_{n=1}^{\infty}\left\{\begin{array}{c}\left[\rho A+M_0\delta(z-z_0)\right]\sin\left(\frac{n\pi z}{L}\right)\ddot{a}_n(t)\\ +\left\{\begin{array}{c}\left(\frac{n\pi}{L}\right)^2\left[kGA-R_0-P_0(t)H(z-z_0)\right]\sin\left(\frac{n\pi z}{L}\right)\\ +\left[P_0(t)\delta(z-z_0)\right]\frac{n\pi}{L}\cos\left(\frac{n\pi z}{L}\right)\end{array}\right\}\\ a_n(t)\\ +jkGA\left[\frac{(n-1)\pi z}{L}\right]\sin\left[\frac{(n-1)\pi z}{L}\right]b_n(t)\end{array}\right\}\\
&=-\rho Ag+\left\{\begin{array}{c}m_0^p e_0\dot{\theta}^2\left[\cos(\dot{\theta}t+\theta_0)+j\sin(\dot{\theta}t+\theta_0)\right]\\ -M_0 g\end{array}\right\}\\
&\delta(z-z_0)\\
&\sum_{n=1}^{\infty}\left\{\begin{array}{c}\left[\rho I+I_0\delta(z-z_0)\right]\ddot{b}(t)-\\ 2j\Omega\left[\rho I+I_0\delta(z-z_0)\right]\dot{b}_n(t)\\ +EI\left[\frac{(n-1)\pi z}{L}\right]^2 b_n(t)+\\ kGAb_n(t)-\\ j\frac{n\pi}{L}kGAa_n(t)\cos\left(\frac{n\pi z}{L}\right)\end{array}\right\}\cos\left[\frac{(n-1)\pi z}{L}\right]\\
&=PRe^{-J\varphi}\delta(Z-Z_0)
\end{aligned}
\tag{13}
$$

By applied Galerkin method Eq.13 is rewritten as:

$$\sum_{n=1}^{\infty}\int_{0}^{L}\left\{\begin{array}{c}\left[\begin{array}{c}\rho A+\sum_{i=1}^{2}M_0\delta(z-z_0)\\ sin\left(\frac{n\pi z}{L}\right)sin\left(\frac{m\pi z}{L}\right)\ddot{a}_n(t)\end{array}\right]+\\ \left\{\begin{array}{c}\left(\frac{n\pi}{L}\right)^2\left[kGA-R_0-P_0H(z-z_0)\right]\\ sin\left(\frac{n\pi z}{L}\right)sin\left(\frac{m\pi z}{L}\right)\\ +P_0\delta(z-z_0)\frac{n\pi}{L}\\ cos\left(\frac{n\pi z}{L}\right)sin\left(\frac{m\pi z}{L}\right)\end{array}\right\}\\ a_n(t)\\ +jkGA\frac{(n-1)\pi}{L}sin\left(\frac{(n-1)\pi z}{L}\right)\\ sin\left(\frac{m\pi z}{L}\right)b_n(t)\end{array}\right\}dz \quad (14)$$

$$=-\rho Ag\int_0^L sin\left(\frac{m\pi z}{L}\right)dz$$

$$+\left\{m_0^p e_0\Omega^2\left[\cos(\Omega t+\theta_0)+jsin(\Omega t+\theta_0)\right]-M_0 g\right\}$$

$$\int_0^L\delta(z-z_0)\sin\left(\frac{m\pi z}{L}\right)dz$$

$$\sum_{n=1}^{\infty}\int_{0}^{L}\left\{\begin{array}{c}\left[\rho I+I_0\delta(z-z_0)\right]\ddot{b}(t)\\ -2j\Omega\left[\rho I+I_0\delta(z-z_0)\right]\dot{b}_n(t)\\ +EI\left(\frac{(n-1)\pi}{L}\right)^2 b_n(t)\\ +kGAb_n(t)-jkGA\frac{n\pi}{L}a_n(t)cos\left(\frac{n\pi z}{L}\right)\end{array}\right\}$$

$$\cos\left[\frac{(m-1)\pi z}{L}\right]dz=PRe^{-J\varphi}\int_0^L cos\left(\frac{(m-1)\pi z}{L}\right)$$

$$\delta(Z-Z_0)dz$$

The simplified form is briefed as:

$$[M]\left\{\ddot{X}(t)\right\}+[C]\left\{\dot{X}(t)\right\}+[K(t)]\{X(t)\}=[F(t)] \quad (15)$$

3- Numerical Results and Discussion

3- 1- Free vibration

In order to determine the forward and backward rotor frequencies for free vibration, we have the following definitions:

$$u(z,t)=\sum_{n=1}^{\infty}a_n e^{j\omega t}\sin\frac{n\pi z}{L}$$

$$\varphi(z,t)=\sum_{n=1}^{\infty}b_n e^{j\omega t}\cos[\frac{(n-1)\pi z}{L}] \quad (16)$$

In this regard, ω is the natural frequency of the whirling. By applied Galerkin method can be written:

$$\left(\omega^2[M]+\omega[C]+[k]\right)\{X\}=\{0\} \quad (17)$$

In order to obtain an unbiased zero response in (17), the determinants of the coefficients must be zero; in other words:

$$\left|\omega^2[M]+\omega[C]+[k]\right|=0 \quad (18)$$

By using equation (18), the natural frequencies will be obtained for the motion of the whirling. Given the coherent coefficients in the stiffness matrix, all the roots of the equation will be purely imaginary, and they will result in forward and backward frequencies.

Initially, a rotor of length L=3 m and diameter d=40 mm without axial force was investigated, the results of which are shown in the form of Campbell diagram for the first and second modes in Figs. 3 and 4.

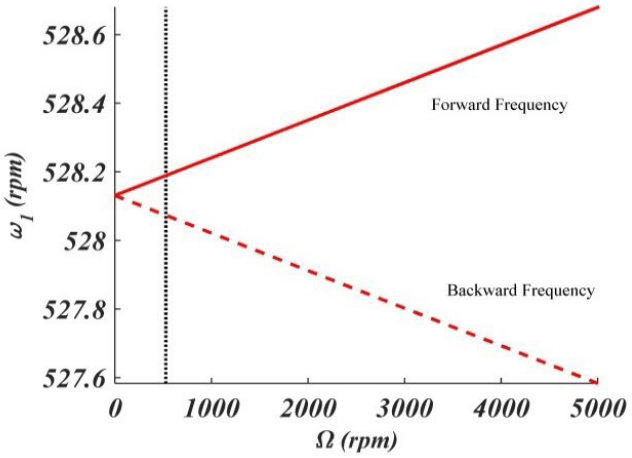

Fig. 3. The Campbell diagram of the first mode of rotor without force with *d*=40mm

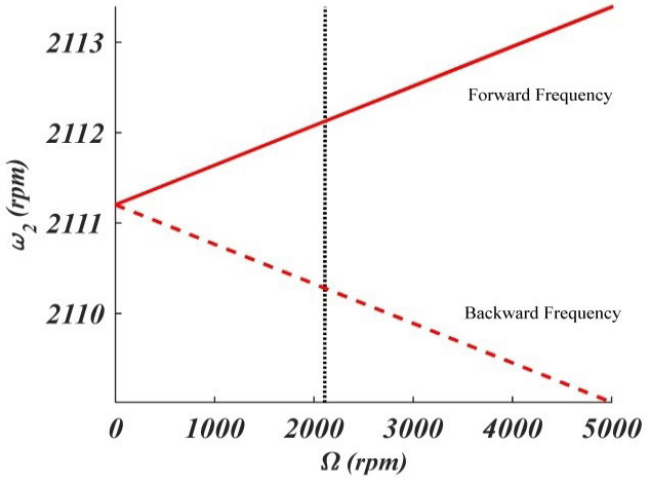

Fig. 4. The Campbell diagram of the second mode of rotor without force with *d*=40mm

Also for d=60mm corresponding Campbell diagram are depicted in Figs. 5 and 6.

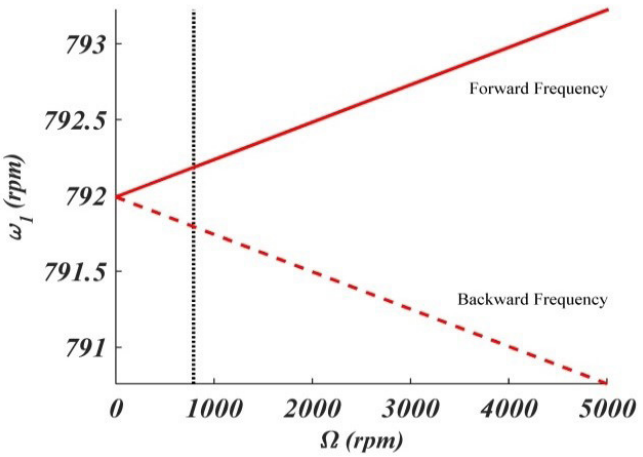

Fig. 5. The Campbell diagram of the first mode of rotor without force with *d*=60mm

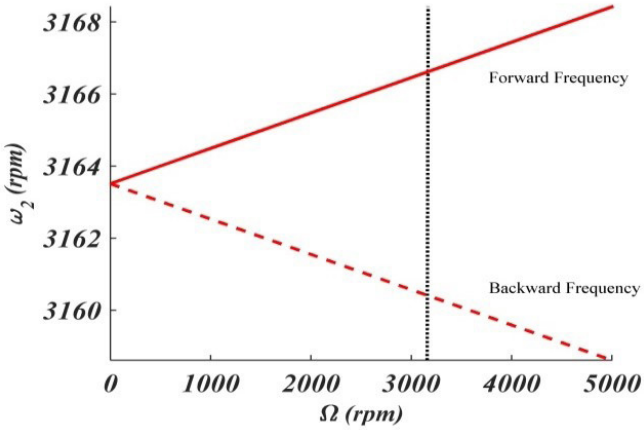

Fig. 6. The Campbell diagram of the second mode of rotor without force with *d*=60mm

As can be seen, the frequency increases as the diameter increases.

In order to investigate effect of axial forces on Campbell diagrams, we apply force 100000 N/m^2 in the middle of the rotor. The obtained results are shown in Figs. 7and 8.

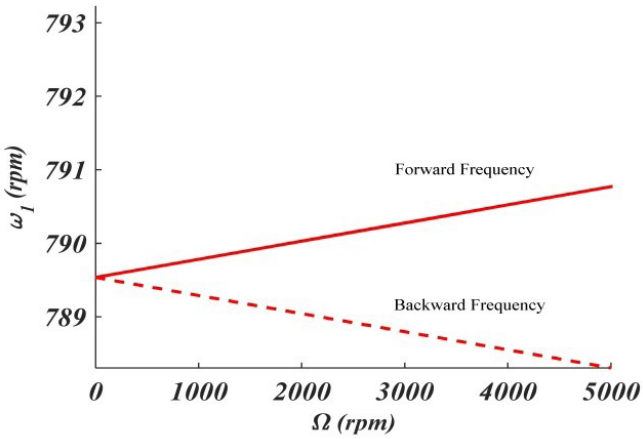

Fig. 7. The Campbell diagram of the first mode of rotor with a force of 100,000 N/m^2 (*d*=60mm)

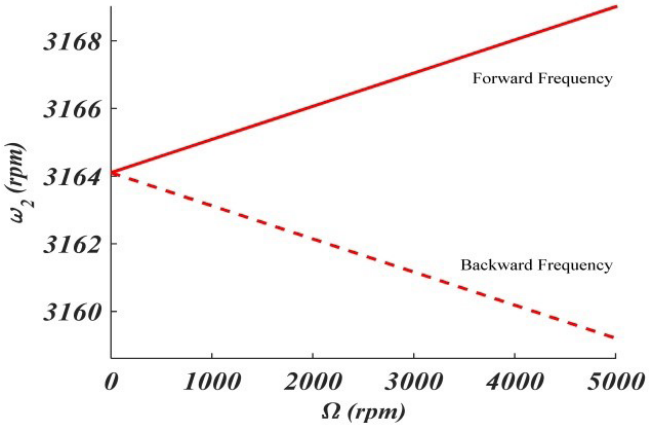

Fig. 8. The Campbell diagram of the second mode of rotor with a force of 100,000 N/m^2 (*d*=60mm)

Applying this force will decrease the frequency of the system in the first mode. Also, in the second mode the system frequencies begin to increase. These trends depend on the position of the force. There exists an appropriate agreement between results of this study and [8].

3- 2- Forced vibration

In order to present and analyze the results obtained in this study, some specifications of the subject rotor are selected from Table 1.

Table 1. Considered rotor characteristics

Characteristics	Value	Symbols & dimensions
Rotor diameter	50	d (mm)
Rotor length	4	L (m)
Modulus of elasticity	200	E (GPa)
Poisson's ratio	0.3	υ
Density	7860	ρ (Kg/m^3)
Location of disk	$L/2$	z_0
Mass of disk	5	M_0 (Kg)
Moment of inertia	2	I_0 (Kg.m^2)
Unbalance mass	10	m_0^p (gr)
Unbalance radios	50	e_0 (mm)
Unbalance angle with x direction	45	θ_0 (degree)
Rotational speed	50	Ω (rpm)

In order to examine the accuracy of the drawn up codes, the rotor was first modeled as a simple beam without rotation, while the results were compared with the accurate solution to the problem. The results were then obtained through assuming α=1/2, β=1/4 and Δt=0.01 in Newmark-beta solution [13] and by taking into accounts the first five sentences of Galerkin solution (N_i=5) by coding in the MATLAB software.

Given that there is no reference to verify the results, modeling method and the drawn up codes, the axial force, and the rotor's rotation were removed; and merely a model of the beam with a simple support was taken into account. Therefore, the extent of motion at the left support and the shear force along x axis

in the left support of the rotor were calculated and shown in Figs. 9 and 10.

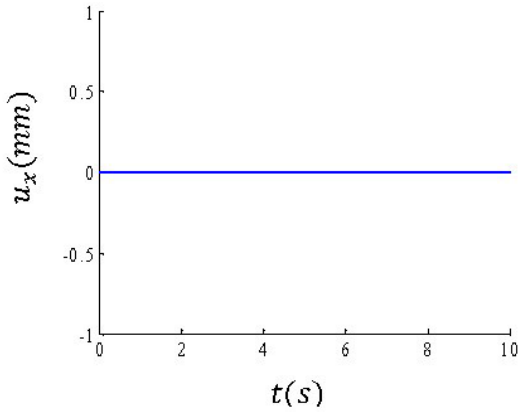

Fig. 9. Displacement in the left support (x direction)

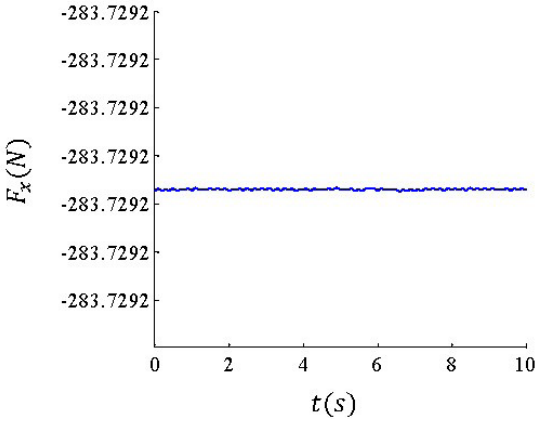

Fig. 10. Shear force in the left support (x direction)

The results have reveals that a constant force of approximately 284 Newton is exerted on the left support. The extent of motion at the rotor's left support is zero corresponding to that of the system. The error percentage among values and their analytical solutions found hear are tabulated and compared in Table 2. The result of the analytical solution is obtained from the static solution and the material strength .There exists an appropriate agreement between results and the drawn up codes of this study and [14].

Table 2. Comparison between the present method and the analytical results

Parameter	Analytical solution	Present solution	Error percentage
F_x, N	301	284	5.7

To confirm the procedure applied in rotor rotation we will consider a rotor with a disk in the middle with the given specifications is considered. The resulting displacement is equal with a simple Jeffcott model. where, the rotor's will be modeled with a mass and spring to a degree of freedom. The equations governing the Jeffcott rotor in two directions is expressed as follows [15]:

$$M_{eff}\ddot{u}_x + k_x u_x = m_0^p e_0 \Omega^2 \cos(\Omega t + \phi_0) \tag{19}$$

$$M_{eff}\ddot{u}_y + k_y u_y = m_0^p e_0 \Omega^2 \sin(\Omega t + \phi_0)$$

Which we have in these equations:

$$M_{eff} = M_0 + \frac{1}{2}M_{rotor}$$
$$k_x = k_y = \frac{48EI}{L^3} \tag{20}$$

The displacement diagram in x directions of this study against Jeffcott model is compared in Fig. 11.

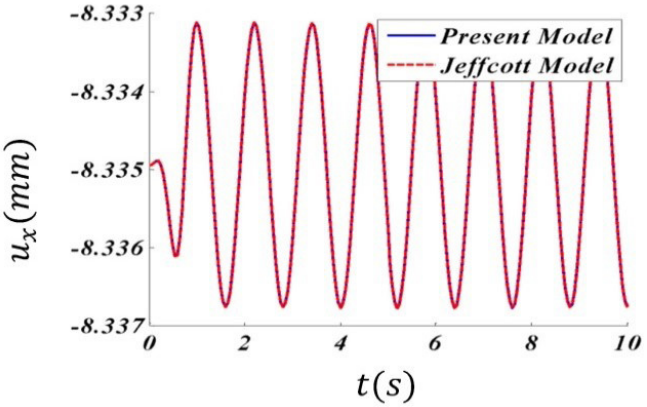

Fig. 11. Displacement in the middle of the rotor (x direction)

The high compatibility of this model with the Jeffcott model is observed in the same figure.

In order to study the effects of axial load on the responses, a harmonic axial load on the disk is considered with an amplitude and frequency of 20 kN and 5 rad/s, respectively, at a radius of 30mm and a 45° angle to the horizontal direction. The shear force at the left support for the unbalanced rotor with axial harmonic force of p=20sin(5t) is shown in Fig.12.

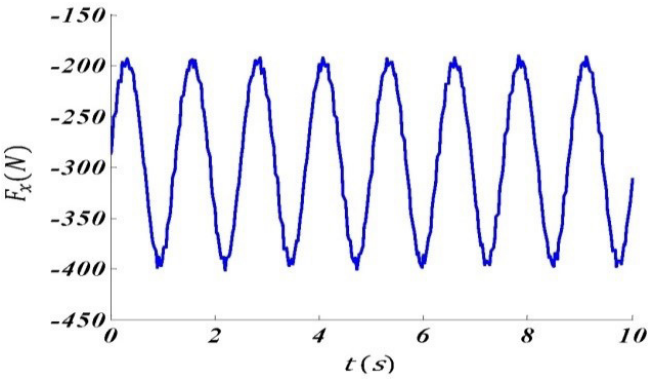

Fig. 12. Shear force in the left support (x direction)

The displacement in the middle of the rotor in the x direction is shown in Fig. 13.

The bending moment in the middle of the rotor in the y direction is shown in Fig. 14.

As observed in this set up the average value of the shear force in the support is increased and oscillated due to both the unbalanced and horizontal forces. In order to check the effect of increased horizontal force the amplitude of the same is increased here.

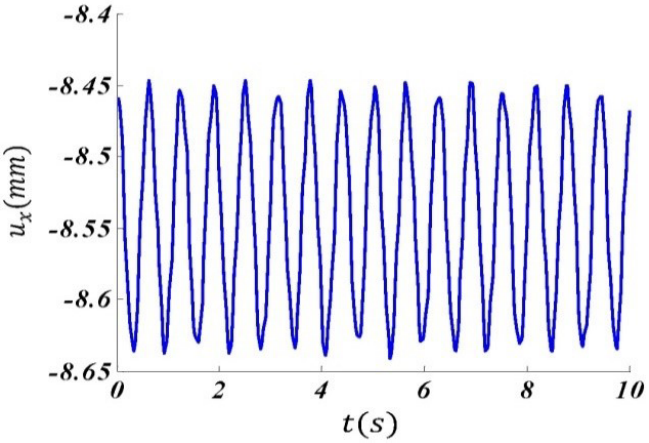

Fig. 13. Displacement in the middle of the rotor (x direction)

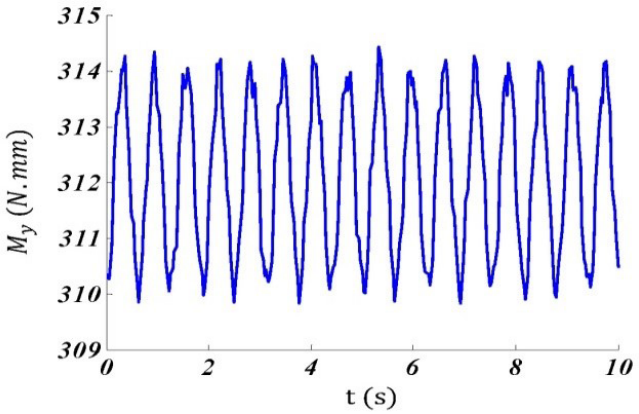

Fig. 14. Bending moment in the middle of the rotor (y direction)

As to the unbalanced rotor with axial harmonic force of p=20sin(5t) the obtained results are shown in Figs.15-17.

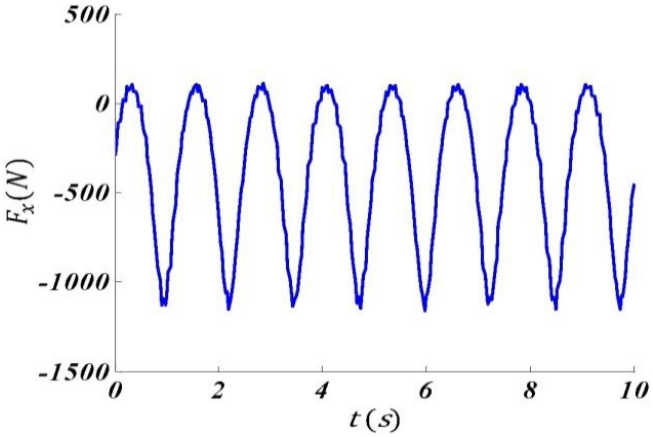

Fig. 15. Shear force in the left support (x direction)

As observed there exists a direct relation between horizontal and shear forces. In this case, the force average value is around 600 N which can rise up to about 1,100 N. This result can be applied in designing the bearings of the system. The amount of displacement and bending moment in the center of the rotor increase. An increase in rotor displacement can cause rotor and stator contact, thus, a problem in the system.

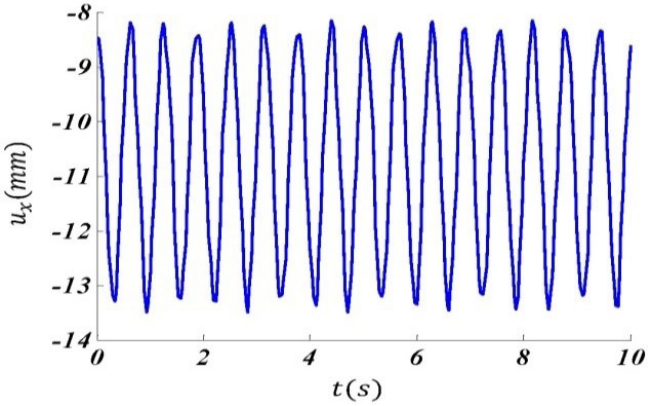

Fig. 16. Displacement in the middle of the rotor (x direction)

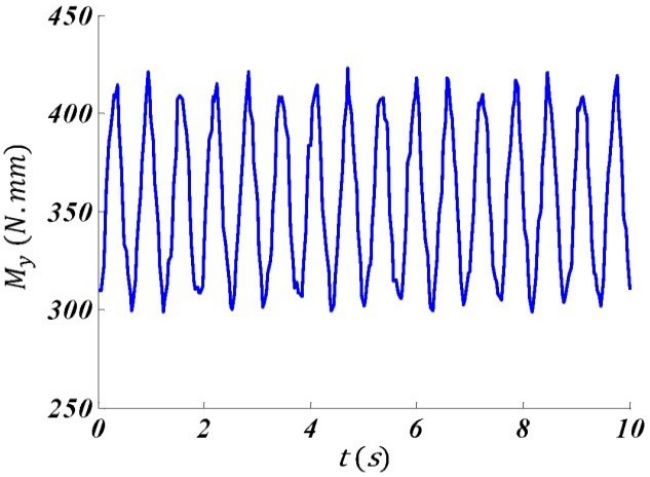

Fig. 17. Bending moment in the middle of the rotor (y direction)

In general, these results indicate which forces are created horizontally the effects of stall and surge can increase the amplitude of rotor lateral vibrations. Consequently, by measuring the vibrations in the bearing of the system, it is possible to detect the occurrence of these phenomena because they can lead to system failure.

4- Conclusions

The effect of axial concentrated forces on lateral vibration of a rotating shaft of the disk with central mono-disk is analyzed. This rotor is assumed to be uniform and the Timoshenko theory is adopted here. The partial differential equations of motion are derived through equilibrium equations for an element of the rotor. The rotor is a simply supported one and the Galerkin-Newmark method is adopted directly in the partial differential equations of motion. The results show that the application of horizontal force in a rotor causes a change in the critical speed of the system. Responses of the lateral vibration for with and without axial force are analysed, and it is observed that an increase in the amplitude of force leads to an increase in the amplitude and mean value of the shear force in the support, displacement and bending moment in the center of the rotor. The results can be applied in analyzing the phenomenon of surge and stall in gas turbines. If the forces at supports are measured and the changes thereof of concern, then, these phenomena could be identified.

References

[1] A. Musznynska, *Rotor dynamics*, Crc press, Taylor Francis Group, LLC. 2005.

[2] H.D. Nelson, A finite rotating shaft element using Timoshenko beam theory, *Journal of Mechanical Design*, 102(4) (1980) 703-803.

[3] S.L. Edney, C.H.J. Fox, E.J. williams, Tapered Timoshenko finite elements for rotor dynamics analysis, *Journal of Sound and Vibration*, 137(3) (1990) 463-481.

[4] S. Chen, M. Geradin, Exact and direct modeling earing systemtechnique for rotor-bs with arbitrary selected degress-of-freedom, *Shock and Vibration*, (1994) 497-506.

[5] S.H. Choi, C. Pierre, A.G. Ulsoy, Consistent modeling of rotating Timoshenko shafts subjected to axial loads, *Journal of vibration and acoustics*, 114(2) (1992) 249-259.

[6] M. Ouyang, M. Wang, A dynamic model for a rotating beam subjected to axially moving forces, *Journal of Sound and Vibration*, 308 (2007) 674-682.

[7] A. Askarian, S.M.R. Hashemi, Effect of axial force, unbalance and coupling misalignment on vibration of a rotor gas turbine, *14 th International Congress on Sound Vibration*. Australia, 2007.

[8] M. Nawal, A.L. Raheimg, Free vibration of simply supported beam subjected to axial force, *Journal of Babylon University*, 2012.

[9] A.A. Motallebi, M. Poorjamshidian, Vibration analysis of a nonlinear beam under axial force by homotopy analysis method, *Journal of Solid Mechanics*, 6 (2014) 289-298.

[10] K. Torabi, H. Afshari, Exact solution for whirling analysis of axial–loaded Timoshenko rotor using basic functions, 4 (2015) 97-108.

[11] G. Genta, *Dynamics of rotating systems*, Springer Science & Business Media, 2007.

[12] J. R. Hutchinson, Shear cofficients for Timoshenko beam theory, *Journal of Applied Mechanics*, 68(1) (2001) 87-92.

[13] N.M. Newmark, A method of computation for structural dynamics, *Journal of the engineering mechanics division*, 85 (1959) 67-94.

[14] G. Bassin, S.M. Brodsky, H. Wolkaff, *Statics and Strength of Materials*, McGRAW-Hill Book Company, 1979.

[15] J. Vance, F. Zeidan, B. Murphy, *Machinery Vibration and Rotor Dynamics*, John Wiley & sons, INC, 2010.

Please cite this article using:

M. R. Zeinolabedini and M.Rafeeyan, The Effect of Concentrated Axial Harmonic Force on the Response of Lateral Vibration for a Jeffcott Rotor, *AUT J. Mech. Eng.*, 2(1) (2018) 91-98.

DOI: 10.22060/ajme.2018.12951.5485